

Experimental determination of the electrical band-gap energy of porous silicon and the band offsets at the porous silicon/crystalline silicon heterojunction

F. P. Romstad and E. Veje

Oersted Laboratory, Niels Bohr Institute, Universitetsparken 5, DK-2100 Copenhagen, Denmark

(Received 12 August 1996; revised manuscript received 21 October 1996)

Photovoltaic and photocurrent measurements have been carried out on a series of samples consisting of porous silicon on top of crystalline silicon. From the experimental data set, the electrical band-gap energy of porous silicon is deduced to be (1.80 ± 0.02) eV, and the conduction-band and valence-band offsets at the porous silicon/crystalline silicon heterojunction are determined to be (0.12 ± 0.01) eV and (0.57 ± 0.03) eV, respectively. The results are compared to previous determinations and discussed. [S0163-1829(97)00408-6]

I. INTRODUCTION

Photoluminescence (PL) properties of porous silicon (PS) have for the past few years been studied intensively, because PS can emit very bright PL even at room temperature, in great contrast to crystalline silicon (*c*-Si), which is a semiconductor with an indirect band gap. Overviews of experimental and theoretical works on PS, with references to preceding review articles can be found in Refs. 1 and 2, respectively.

PS has in a recent work from our laboratory been studied in detail with a combination of PL, photoluminescence excitation, and photoabsorption.³ The data indicated that the PL is of molecular nature, and the optical band-gap energy of PS was measured to be 1.59 eV or larger, depending on sample preparation. In addition, the energy-band diagram related to the PL was constructed.³ In contrast to the large number of works on the PL properties of PS, the electric and also photoelectric properties of PS have been studied only sporadically, cf. Refs. 1, 2. Therefore, we have produced a series of heterostructures, each consisting of a fairly thick layer of PS on top of the *p*-type *c*-Si wafer, on which it was grown, and studied transverse photovoltaic effects together with photocurrent (PC) through these samples. With photocurrent we mean electric current induced above its dark current level by photon illumination.

II. EXPERIMENT

The samples were produced by etching *p*-type *c*-Si wafers electrochemically in hydrofluoric acid mixed with ethanol, 1:1. The electrolytic cell used for the etchings, and the etching procedure are described in Ref. 3. The *c*-Si wafers used were of crystal orientation (100), and were fairly lightly doped ($1\text{--}30 \Omega \text{ cm}$). Samples were produced with different current densities, from 5 mA/cm^2 to 25 mA/cm^2 , and the current density was always kept constant during etching. Etching times were from 60 to 90 minutes, so that in each case, a fairly thick layer of PS was produced. This was of importance, to avoid direct contact from the electrode on the top surface of the PS film to the *c*-Si wafer. In all cases, the PS layer remained on the *c*-Si wafer on which it was produced. No attempts have been done here to carry out measurements on self-supporting films of PS.

After production, the samples were dried and stored in air at room temperature for several days, before measurements were carried out on them. Each sample was mounted on a copper plate by gluing the back side of the *c*-Si wafer to the copper plate with the use of a drop of silver paste. This served two purposes, namely, to create good electrical contact between the copper and the back of the *c*-Si wafer, and also to fix the sample to its holder.

The following three types of electrical contacts were used at the top surface of the PS layer. (i) A thin (10–20-nm-thick) semitransparent gold layer was vacuum evaporated onto the surface. (ii) The end of a thin metal wire was glued onto the PS surface with a droplet of silver paste. (iii) A flat, metal spring leave was gently pressed towards the PS surface. All three types of contacts were stable in time and yielded reproducible results. The data sets obtained with the three types of contacts were identical on relative scales.

As illumination, a 250-W halogen lamp coupled to a McPherson model 207 scanning monochromator ($f=0.67 \text{ m}$) was used, different spectral orders being separated by appropriate filters. A bifurcated optical cable was mounted at the exit slit of the monochromator in such a way, that the sample could be illuminated by one of the cable outputs, while the other output was coupled to an optical power meter. In this way, the illumination of the sample could be monitored continuously without interrupting illumination of the sample, which was placed in an otherwise light-sealed metal box, shielding it from external electric noise. The power of the monochromatic light from the monochromator was a few μW . The short-wavelength limit, 400 nm, was set by absorption in the glass fibers below this wavelength. All data reported here have been taken at room temperature.

The current through the sample was measured with a picoammeter with dark current suppression and with an analog output connected simultaneously to a chart recorder and a personal computer with adequate hardware and software. This way, slow variations (time scales of days or longer) could be registered with the use of the chart recorder, and faster changes could be observed with the computer with an overall time resolution limit of 1 ms.

All data have been normalized to same photon fluence. The geometrical sizes of the samples were not determined. Therefore, all of the data presented are on relative scales.

The samples were studied with PL at room temperature,

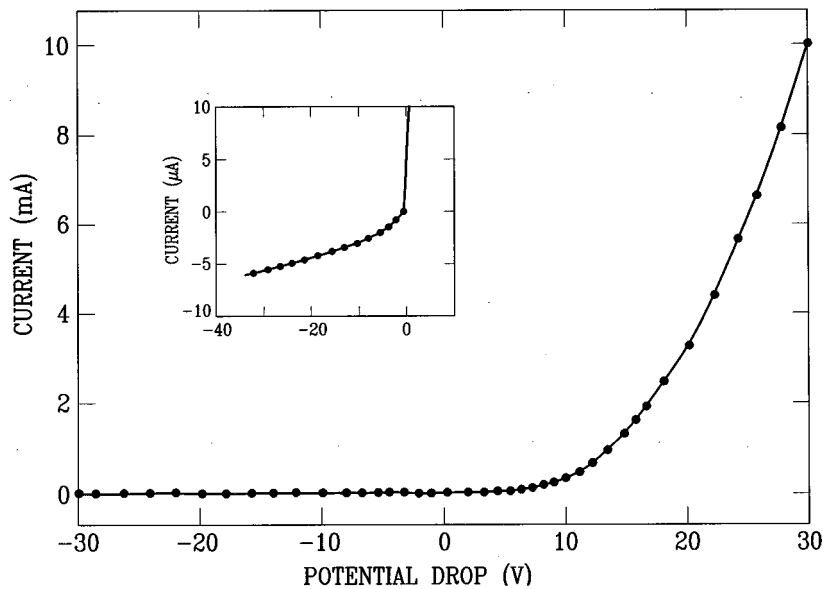


FIG. 1. Typical data for the current through a sample versus the potential drop across the sample. The measurements were taken without exposing the sample to light. The inset shows the current versus potential drop in the reverse direction with the current scale enlarged.

as well as at 10 K, at the PL facility described in Ref. 3. At room temperature, the maxima in PL intensity were in the wavelength region 750–780 nm, which indicated that the samples had a fairly high content of hydrogen, as estimated with the use of Fig. 4 in Ref. 4. No annealing or other preparation treatment were carried out on the samples after growth, except that they were stored in air at room temperature approximately one week or more before they were used. Some of the samples were studied repeatedly over a period of a couple of months and showed no changes.

III. RESULTS AND DISCUSSION

A. Current-voltage characteristics

Current-voltage (I - V) characteristics were measured for samples without illumination. A typical result is shown in Fig. 1, in which a rectifying behavior is seen clearly. For all samples, in the forward direction, the positive output of the external power supply was connected to the c -Si wafer, and the negative output to the PS layer. It is worth noting, that typically, the samples could withstand a high potential drop without breakdown, and also, that the current in the reverse direction was very reduced as compared to the forward direction. As an example, in Fig. 1, the ratio between the currents in forward and reverse directions is 2×10^3 , measured with 30 V across the sample. Similar rectifying behavior of PS/ c -Si heterojunctions has been reported previously.^{5–8} This rectifying behavior is discussed at the end of Sec. III C in the light of the band-structure results presented in Secs. III B and III C.

B. Photovoltaic results

If a semiconductor structure has an internal electric field, then the electron-hole pairs generated by photon absorption can be separated by the internal field, and this can produce a measurable potential drop across the sample and/or a current in an external circuit. This is the photovoltaic effect; for an overview, see, e.g., Ref. 9.

Our samples produced measurable photovoltaic signals which, albeit being of the order of a few μ V or nA, clearly

were discernible from the noise level. Also, they were reproducible, and different samples showed the same relative spectral shape.

The photovoltaic charge separation was always such that in the sample, photoexcited electrons moved towards the front surface of the PS layer, and holes moved towards the c -Si backing. In other words, for the photovoltaic effect, the motions of photocreated charge carriers through the samples were identical to the flows when an external power supply was applied in the reverse direction.

In Fig. 2 are shown typical photovoltage data (upper curve) and photocurrent data (lower curve) versus the wavelength of the illuminating light (bottom scale) and the photon energy (top scale). The similarities between the two curves in Fig. 2 are striking. For both curves, a clear onset is observed at 689 nm, corresponding to 1.80 eV. At wavelengths above this onset, very weak signals were seen up to approximately 950 nm (1.30 eV), and nothing could be detected above this wavelength. Our interpretation is that the photon energy at the onset is identical to the electrical band-gap energy of PS. The average value for this energy, obtained as an average of all of our results, is (1.80 ± 0.02) eV.

In the data reduction, the relevant sections of the curves were extrapolated to zero signal with the use of straight lines, as indicated in Fig. 2, and the onset energy was identified as the position of zero signal. The uncertainty quoted accounts for uncertainties in the extrapolation procedure.

Concerning whether we deal with a direct or an indirect band gap, we mention the following. The variation of the absorption constant with photon energy in the region slightly above the threshold depends on the nature of the band gap; for a discussion, see, e.g., Ref. 9. For the bulk of an ideal semiconductor with direct band gap, the square of the absorption constant is proportional to the difference between the photon energy and the band-gap energy.⁹ For an ideal, bulk semiconductor with indirect band gap, a plot of the square root of the absorption constant consists⁹ of two straight lines, one corresponding to absorption of a phonon, and the other to emission of a phonon. By transforming the signals presented in Fig. 2 to signal versus photon energy

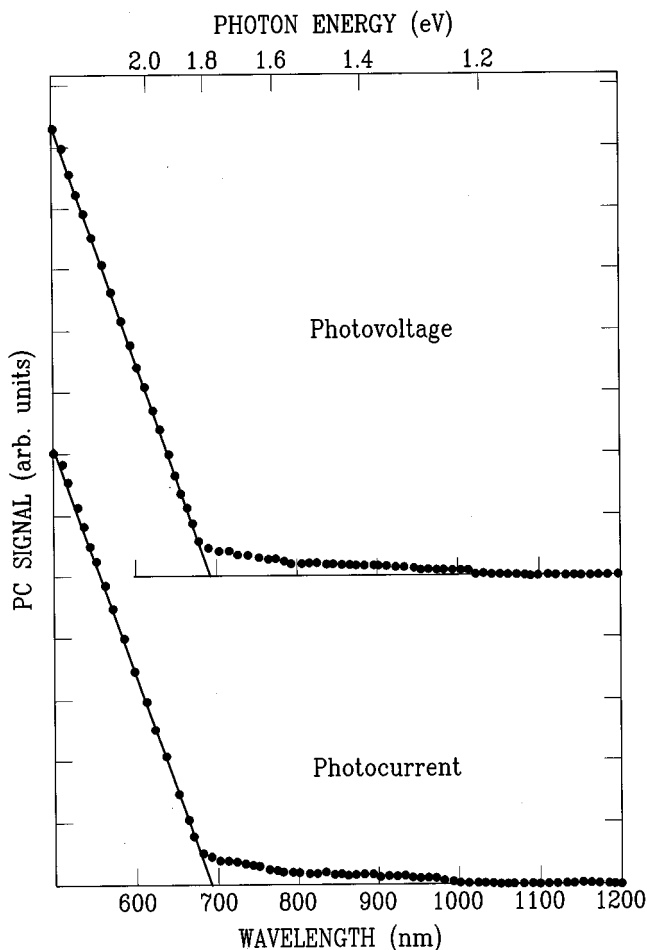


FIG. 2. Typical curves for illumination-induced photovoltage (upper curve) and photocurrent (lower curve) plotted vs the wavelength (lower scale) and photon energy (upper scale) of the illuminating light. The measurements were taken without an external potential applied to the sample.

instead of wavelength, none of the two above-described behaviors were observed. This need not be a surprise, because the descriptions in Ref. 9 apply to the ideal cases of bulk semiconductors, and we deal with fairly thin films, which are very inhomogeneous in thickness. However, we observed no trace of a variation consisting of two components, one corresponding to phonon absorption, and the other to phonon emission. This seems to indicate that the PS samples we have been working with have a direct band gap. Further support for a direct-gap nature of PS comes from the blueshift of the photoluminescence from PS with increasing hydrostatic pressure¹⁰ as well as from the observation of very bright electroluminescence from PS (see, e.g., Ref. 1). At the same time we mention that a question as to whether the band-gap nature of PS is direct or indirect may be a wrongly posed question, because long-range order is lost in PS and therefore, the k vector and thus the concept of a direct or indirect gap no longer have any precise meaning. Therefore, we assume that photovoltaic processes as those shown in Fig. 2 are not phonon assisted. Consequently, the band-gap energy as given above does not need a phonon-energy correction.

In the work by Andersen and Veje,³ a kink was observed at approximately 650 nm in the absorption curve and also in

all photoluminescence excitation curves recorded. At shorter wavelengths, all such curves had a steeper slope than at wavelengths above approximately 650 nm. If the sections of these curves below 650 nm are extrapolated to zero signal, a threshold is found at a photon energy of 1.80 eV. In other words, in Ref. 3, all curves which are measures of photoabsorption in PS indicate a change in the photoabsorption at a photon energy identical to what is observed here, namely 1.80 eV. For photon energies above 1.80 eV, the absorption is larger than below this energy, indicating a band edge at 1.80 eV. Thus, the photoabsorption studies in Ref. 3 conform with the value for the electrical band-gap energy for PS, as derived from the photovoltaic work.

The very weak signal observed above 689 nm (cf. Fig. 2) decreased gradually for increasing wavelength, and disappeared at around 950 nm. We were unable to observe a clear threshold, due to poor signal-to-noise ratio. One probable interpretation is that this weak photoinduced signal is caused by photoexcitations from surface-related states and/or in discrete levels in the band gap.

C. Photocurrent results with external bias applied

With an external power supply connected to the sample in the reverse direction, PC's could readily be detected. Two typical PC data sets are shown in Fig. 3 as functions of the wavelength of the illuminating light (bottom scale) and the photon energy (upper scale). Before discussing these results, we mention that time-varying PC and also persistent PC, both with slow relaxation times, have been reported for PS (Ref. 11), but the data reported here have all been obtained so fast and with so low illumination intensities, that all results presented here are undisturbed by such effects with long relaxation times. Only PC signals with a time response shorter than that of the equipment (i.e., 1 ms) are presented and discussed here.

In Fig. 3, three features are seen, at 689 nm (1.80 eV), 1050 nm (1.18 eV), and at 1165 nm (1.06 eV). Different samples showed these three features at the listed wavelengths, independent of sample, and the positions of the three onsets were unaffected by the value of the externally applied potential drop across the samples, cf. Fig. 3. However, the curve shape depended on the external bias in the sense that for large values of the potential drop across the sample, a local maximum was seen at around 940 nm, whereas for small potential drops, the PC curve was rather flat in this wavelength region, see Fig. 3.

In the data analyses, the relevant sections of the PC spectra were fitted with straight lines, as indicated in Fig. 3, and the onset energies were identified as the positions of the crossing points between the straight lines. The uncertainties quoted account for the overall uncertainties related to this procedure. The energy values listed in the following are average values obtained from different samples and also with different values of the externally applied potential drop.

The threshold observed at (1.80 ± 0.02) eV is evidently the same as that discussed in Sec. III B. Thus, we shall here offer the same interpretation as that given in Sec. III B, namely, that the photon energy at this onset equals the electrical band-gap energy of PS, and refer the reader to the discussion given in Sec. III B.

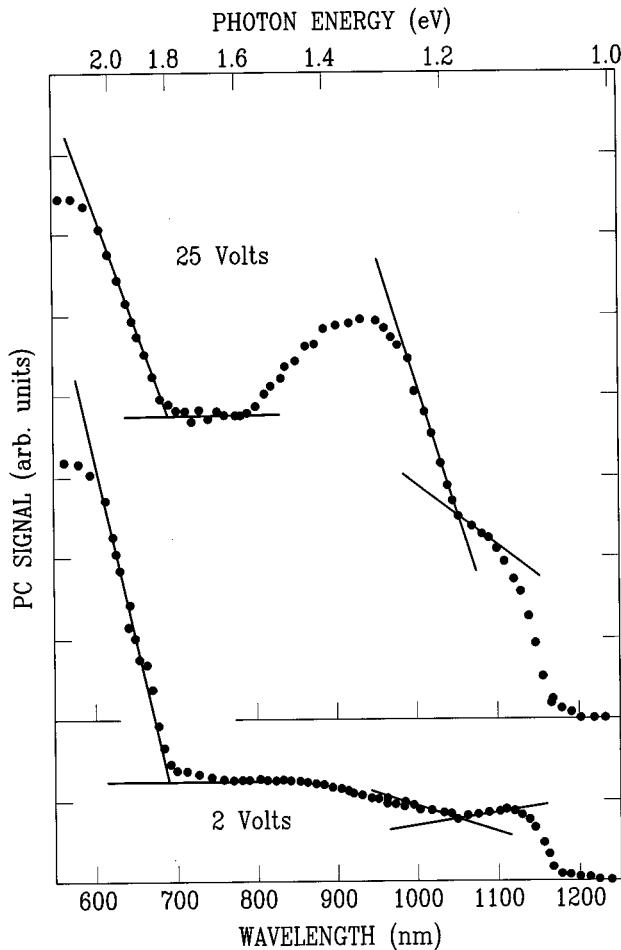


FIG. 3. Typical PC signals in arbitrary units plotted vs the wavelength (lower scale) and photon energy (upper scale) of the illuminating light. The upper curve was recorded with 25 V across the sample, and the lower curve with 2 V across the sample.

The onset seen at (1.064 ± 0.005) eV is located at a photon energy, which is identical to the difference between the band-gap energy of *p*-type *c*-Si at room temperature¹² and the boron acceptor-level energy in *c*-Si (taken from Ref. 13). The interpretation that the onset at 1.064 eV is caused by PC in *c*-Si was confirmed by carrying out PC measurements on unetched *p*-type *c*-Si samples, which yielded a strong response with a relative curve shape as that seen in the wavelength region 1100–1200 nm in Fig. 3. The presence of a PC signal which is traceable to only *c*-Si is most presumably caused by small sections of the samples where the electrical contact on the top surface was directly connected to the *c*-Si wafer, thus shortening out the PS layer. The relative height of the signal from pure *c*-Si, as compared to the rest of the PC spectrum, changed from sample to sample, also in case different samples had been grown together on the same wafer.

The PC response observed at 1050 nm in Fig. 3 corresponds to a photon energy of (1.180 ± 0.008) eV, which according to the previous discussion is below the electrical band-gap energy of PS. Therefore, it must be traceable to photoexcitation taking place in the *c*-Si wafer. However, it was not observed in PC measurements carried out on pure *c*-Si. Consequently, it must also be related to some energy

property of the PS, or rather, to the heterojunction between the layers of PS and *c*-Si. Here, we offer the explanation that it is caused by electrons, which are photoexcited in the *c*-Si backing layer and subsequently, due to the electric field, are injected ballistically from the *c*-Si layer into the conduction band in the PS layer. This way, they will give rise to an electric current. This interpretation is supported by the fact that the relative size of the onset at 1050 nm increases with an increasing external electric potential drop across the sample, cf. Fig. 3, because the higher the field strength will be, the larger such a ballistic injection will be. Also, nothing was observed in this wavelength region in the photovoltaic measurements described in Sec. III B (cf. Fig. 2), in which no external bias was applied to the sample, and consequently, no externally applied force would act on electrons photoexcited in the *c*-Si layer and force them towards the PS layer. The polarity of the external bias was such that electrons, which were photoexcited in the *c*-Si layer would move towards the PS layer, whereas the corresponding holes would move away from the PS layer. Thus, a ballistic injection can take place for electrons at the conduction-band discontinuity, but not for holes at the valence-band discontinuity. The process is basically an internal photoemission process, and has been observed with GaAs/Al_xGa_{1-x}As heterojunctions.¹⁴⁻¹⁷ It is sketched in Fig. 4, in which the band gap of *p*-type *c*-Si is drawn to the left, and the electrical band gap of PS, derived as described above, is drawn in the middle of the figure. The highest occupied molecular orbital in PS is designated HOMO. To the right in this figure is sketched the energy-band structure related to the PL of PS, as derived and discussed in the work by Andersen and Veje.³ In that work, it was suggested that the two PL-related bands are surface bands. All three energy-band structures in Fig. 4 are on the same scale.

At the heterojunction, there can be so-called band bendings, which can be crucial in the data reduction. This has been discussed in detail in a recent work¹⁸ on GaAs/Al_xGa_{1-x}As heterojunctions in which the reverse process, namely, the ballistic injection of electrons from the semiconductor material of the higher-lying conduction-band edge into the other material, combined with the radiative recombination of such electrons in this material, was used to derive the conduction-band offset, i.e., the discontinuity at the heterojunction. The analogy between the two mechanisms is evident by comparing Fig. 4 to Figs. 1, 3 in Ref. 18. Here, we shall first ignore the possible band bendings, and at the end of this section, a possible influence caused by band bending will be discussed.

The conduction-band offset, ΔE_c , at a heterojunction is defined as the discontinuity in the conduction-band edges at the interface. Correspondingly, the valence-band offset, ΔE_v , is the valence-band discontinuity. These two quantities are included in Fig. 4. Evidently, ΔE_c equals the difference between the photon-energy thresholds to create PC in the heterojunction (process labeled 1 in Fig. 4) and to create PC in a pure *c*-Si sample (process labeled 2 in Fig. 4). In other words, from our results, $\Delta E_c = (1.180 \pm 0.008)$ eV $- (1.064 \pm 0.005)$ eV $= (0.12 \pm 0.01)$ eV. We note here that we could determine both of the thresholds with relatively small uncertainties, and also, that the two photoexcitations (processes 1 and 2 in Fig. 4) initiate from the same energy level in the

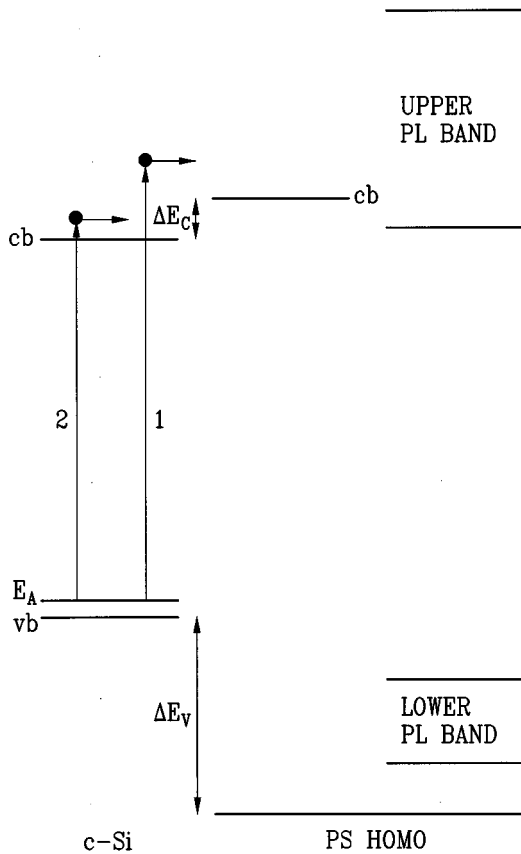


FIG. 4. The figure shows the energy-band structures for *c*-Si (left) and PS (middle and right sections). The band structures are on the same scale, and the band edges have been aligned in accordance with the band-offset determinations described in the text. In the figure are also sketched photoexcitations in *c*-Si followed by a ballistic injection into the PS layer (process 1) and photoexcitations in the *c*-Si layer to energies below the height of the conduction-band edge in PS (process 2).

c-Si. Thus, there is no ambiguity concerning the initial electron energy. The relatively large uncertainty in ΔE_c given above is because ΔE_c results from a difference between two numbers, which are of comparable size.

According to Fig. 4, ΔE_v can be determined from

$$\Delta E_v = E_{PS} - E_{Si} - \Delta E_c,$$

where E_{PS} and E_{Si} are the band-gap energies of PS and *c*-Si, respectively. By using $E_{Si} = 1.109$ eV, as derived from data in Ref. 12, we obtain $\Delta E_v = (0.57 \pm 0.03)$ eV. Again, the relatively large uncertainty stems from differences between comparable numbers.

Now we return to the problem of band bending at the heterojunction. In corresponding works on GaAs/Al_xGa_{1-x}As, such effects manifested themselves in the fact that threshold-energy values were found to depend on the externally applied potential drop, and the extrapolation to zero potential drop was found to be crucial.^{15,18} Here, however, the positions of all three thresholds were independent of the potential drop applied across the sample. From this, we conclude that possible band bendings at the heterojunction are so small that it is justified to ignore them within the

TABLE I. In the table experimental values are presented for the electrical band-gap energy for PS, E_{PS} (first column), the conduction-band offset, ΔE_c (second column), the valence-band offset, ΔE_v (third column), and references to previous works (last column).

E_{PS} (eV)	ΔE_c (eV)	ΔE_v (eV)	Reference
1.80 ± 0.02	0.12 ± 0.01	0.57 ± 0.03	This work
2.20			7
2.9	0.5	1.3	19
1.8	0.3	0.4	20

accuracy of the present work. However, possible band bendings can well be sample dependent, so our findings need not be a common result.

Our results are summarized in Table I, in which also results of other works^{7,19,20} are included. Evidently, agreement between the different data sets is not more than fair. However, the different investigations agree that ΔE_c is smaller than ΔE_v . The results taken from Ref. 20 are average values taken from Fig. 5 in Ref. 20. In that work, a dependence upon preparation parameters was found. Although we searched carefully for a possible dependence on preparation parameters, we failed to observe any. This is worth noting, remembering that our samples were produced under fairly different etching conditions, and also different top contacts were used; cf. Sec. II. In a previous work,³ we studied photoluminescence from PS produced at different etching conditions and arrived at a corresponding conclusion, namely, that with our method to produce PS, the relative photoluminescence spectral distribution depends not very much on production parameters. In Ref. 3 it was concluded that the photoluminescence of PS is of molecular nature, and that it seems quite problematic to account for it with models based on quantum confinements in Si nanostructures (for an overview of such models, see Refs. 1–3). Probably, this is also valid for the photoelectric properties of PS.

In the *p*-type *c*-Si used by us, the Fermi level will at room temperature be close to the acceptor level. When two semiconductor materials form a junction, the Fermi levels in the two materials will in the bulk of them line up to the same horizontal position in a band diagram like that shown in Fig. 4. This rule, if applicable to Fig. 4, will locate the Fermi level in PS to approximately 0.62 eV above the HOMO, i.e., above the upper edge of the lower PL-related band, but almost 0.3 eV below the middle of the band gap of PS. However, PS has at room temperature a very high electrical resistivity. It seems to be a semi-insulating material rather than a semiconductor, and therefore, application of the line-up rule for the Fermi levels is questionable. Nonetheless, the lower PL-related band (Fig. 4) is most presumably below the Fermi level, whereas the upper PL band clearly is above the Fermi level.

Concerning the rectifying behavior described in Sec. III A, it could, in principle, be caused either by the PS/*c*-Si heterojunction or from a Schottky barrier at a contact. When biased in the reverse direction, the positive output from the external power supply is connected to the top of the PS layer, and the negative to the *c*-Si layer; cf. Sec. III A. This implies, that for the contact at the *c*-Si back in itself, the biasing

will be forward,¹³ remembering that the *c*-Si is of *p* type. Also, if holes were injected into the PS layer from the top contact, they would pass through the device, according to Fig. 4. From these considerations, it follows that the rectifying action LS caused by a Schottky barrier at the contact between the top surface of the PS layer and the positive output from the external power supply. This is consistent with the above-given discussion of the position of the Fermi level in the PS layer, according to which the Fermi level is located below the middle of the band gap in PS, because this implies that the PS is of *p* type, and consequently, a Schottky barrier at the top surface would be biased in reverse. The experimental finding that the opposite direction to that just discussed actually is forward, is obviously fully consistent with the energy-band structure shown in Fig. 4 combined with the above-given discussion concerning the reverse direction.

Summarizing briefly, we have carried out photocurrent measurements on PS/*c*-Si heterostructures, and from the

data, we have deduced experimental values for the electrical band-gap energy for PS and the band-edge discontinuities at the interface. The results are presented in Table I. No dependence on etching conditions has been observed. The results are compared to results from a recent optical study³ of PS, and an overall discussion is given with the conclusion that the electrical band gap of PS seems to be direct and an observed rectifying behavior of PS/*c*-Si devices is traceable to a Schottky barrier formed at the metal-PS interface.

ACKNOWLEDGMENTS

This work has been supported by the Danish Natural Science Research Council, the Danish National Agency of Technology, the Carlsberg Foundation, Director Ib Henriksens Foundation, and the NOVO Nordic Foundation. All grants are highly appreciated.

-
- ¹Y. Kanemitsu, Phys. Rep. **263**, 1 (1995).
²G. C. John and V. A. Singh, Phys. Rep. **263**, 93 (1995).
³O. K. Andersen and E. Veje, Phys. Rev. B **53**, 15 643 (1996).
⁴L. Tsybeskov and P. M. Fauchet, Appl. Phys. Lett. **64**, 1983 (1994).
⁵J. P. Zheng, K. L. Jiao, W. P. Shen, W. A. Anderson, and H. S. Kwok, Appl. Phys. Lett. **61**, 459 (1992).
⁶C. Tsai, K.-H. Li, and J. C. Campbell, Electron. Lett. **29**, 134 (1993).
⁷Z. Chen, T.-Y. Lee, and G. Bosman, Appl. Phys. Lett. **64**, 3446 (1994).
⁸V. Pacebutas, A. Krotkus, I. Simkiene, and R. Viselga, J. Appl. Phys. **77**, 2501 (1995).
⁹R. H. Bube, *Photoelectronic Properties of Semiconductors* (Cambridge University Press, Cambridge, England, 1992).
¹⁰J. M. Ryan, P. R. Wamsley, and K. L. Bray, J. Lumin. **60&61**, 378 (1994); J. Zeman, M. Zigone, G. L. J. A. Rikken, and G. Martinez, J. Phys. Chem. Solids **56**, 655 (1995).
¹¹T. Frello, O. Leistiko, and E. Veje, J. Appl. Phys. **79**, 1027 (1996).
¹²C. D. Thurmond, J. Electrochem. Soc. **122**, 1133 (1975); and as quoted in G. E. Jellison, Jr. and D. H. Lowndes, Appl. Phys. Lett. **41**, 594 (1982); and in N. Do, L. Klees, P. T. Leung, F. Tong, W. P. Leung, and A. C. Tam, *ibid.* **60**, 2186 (1992).
¹³S. M. Sze, *Semiconductor Devices, Physics and Technology* (Wiley, New York, 1985).
¹⁴M. Heiblum, M. I. Nathan, and M. Eizenberg, Appl. Phys. Lett. **47**, 503 (1985).
¹⁵G. Abstreiter, U. Prechtel, G. Weimann, and W. Schlapp, Surf. Sci. **174**, 312 (1986).
¹⁶M. Heiblum, M. I. Nathan, and M. Eizenberg, Surf. Sci. **174**, 318 (1986).
¹⁷M. A. Haase, M. A. Emanuel, S. C. Smith, J. J. Coleman, and G. E. Stillman, Appl. Phys. Lett. **50**, 404 (1987).
¹⁸T. Forchhammer, E. Veje, and P. Tidemand-Petersson, Phys. Rev. B **52**, 14 693 (1995).
¹⁹P. H. Hao, X. Y. Hou, F. L. Zhang, and X. Wang, Appl. Phys. Lett. **64**, 3602 (1994).
²⁰Y. Suda, T. Ban, T. Koizumi, H. Koyama, Y. Tezuka, S. Shin, and N. Koshida, Jpn. J. Appl. Phys. **33**, 581 (1994).